Journal of Nanobiotechnology

RESEARCH Open Access

Advancing liver cancer treatment with dual-targeting CAR-T therapy

Ze Yang[1,2,3], Chao Cheng[4], Zhongliang Li[3,5], Huajing Wang[4], Mengmei Zhang[2], Ermin Xie[4], Xu He[1], Bing Liu[1], Hongwei Sun[3], Jiantao Wang[4], Xiaopei Li[4], Dingjie Liu[3], Xiaowen Lin[3], Xianyang Li[4], Ping Jiang[1], Ligong Lu[1,3], Xiaowen He[4*], Meixiao Zhan[1,3*], Ke He[6*] and Wei Zhao[1,3*]

Abstract

Chimeric antigen receptor (CAR)-T cell therapy targeting glypican-3 (GPC3) has shown promise in the treatment of hepatocellular carcinoma (HCC). However, the efficacy of CAR-T cells that focus solely on cell surface tumor-associated antigens is often limited. To overcome this challenge, we developed a dual-targeting CAR-T cell strategy. The intracellular alpha-fetoprotein (AFP) antigen, a well-established biomarker of liver cancer, presents the immunogenic Human Leukocyte Antigen (HLA)-A*02:01-restricted epitope 158–166. Consequently, we engineered a T cell receptor (TCR) mimic antibody with high specificity and affinity, providing a promising therapeutic avenue to target this critical antigen. To enhance treatment outcomes for liver cancer, we further modified previously developed GPC3 CAR-T cells, which demonstrated robust anti-tumor efficacy against GPC3-high tumor cells, to secrete an optimized bispecific T cell engager (BiTE) targeting the presented AFP antigen. This dual-targeting strategy significantly improved CAR-T cell proliferation and persistence, as well as enhancing cytokine expression and anti-tumor activity against HCC cells, particularly those exhibiting low GPC3 and AFP expression, both in vitro and in vivo. Our findings highlight the potential of this innovative approach to offer more effective treatment options for patients with liver cancer.

Introduction

The prevalence of liver cancer is significantly influenced by the high incidence of hepatitis B infection globally. This situation is exacerbated by the poor prognosis associated with liver cancer, as conventional treatment modalities have demonstrated limited effectiveness [1–4].

*Correspondence:
Xiaowen He
peterhe@oricell.com
Meixiao Zhan
zhanmeixiao1987@126.com
Ke He
hiker00006@126.com
Wei Zhao
zhaoweismu@foxmail.com

Full list of author information is available at the end of the article

Recent advancements in immunotherapy have improved survival rates for liver cancer patients. Specifically, the combination of atezolizumab and bevacizumab has been associated with longer overal and progression-free survival compared to sorafenib treatment [5–7]. However, the overall survival rates remain unsatisfactory, particularly for patients with advanced liver cancer [8–10].

In recent years, cellular immunotherapy, particularly CAR T-cell therapy, has emerged as a promising approach for treating solid tumors, showcasing optimistic clinical prospects. Glypican-3 (GPC3), a glycoprotein highly expressed on the surface of liver cancer cells, plays a crucial role in mediating various signaling pathways that influence tumor cell proliferation, differentiation, adhesion, and metastasis. Its selective expression in liver cancer has led to its exploration in developing

Graphical sbstract

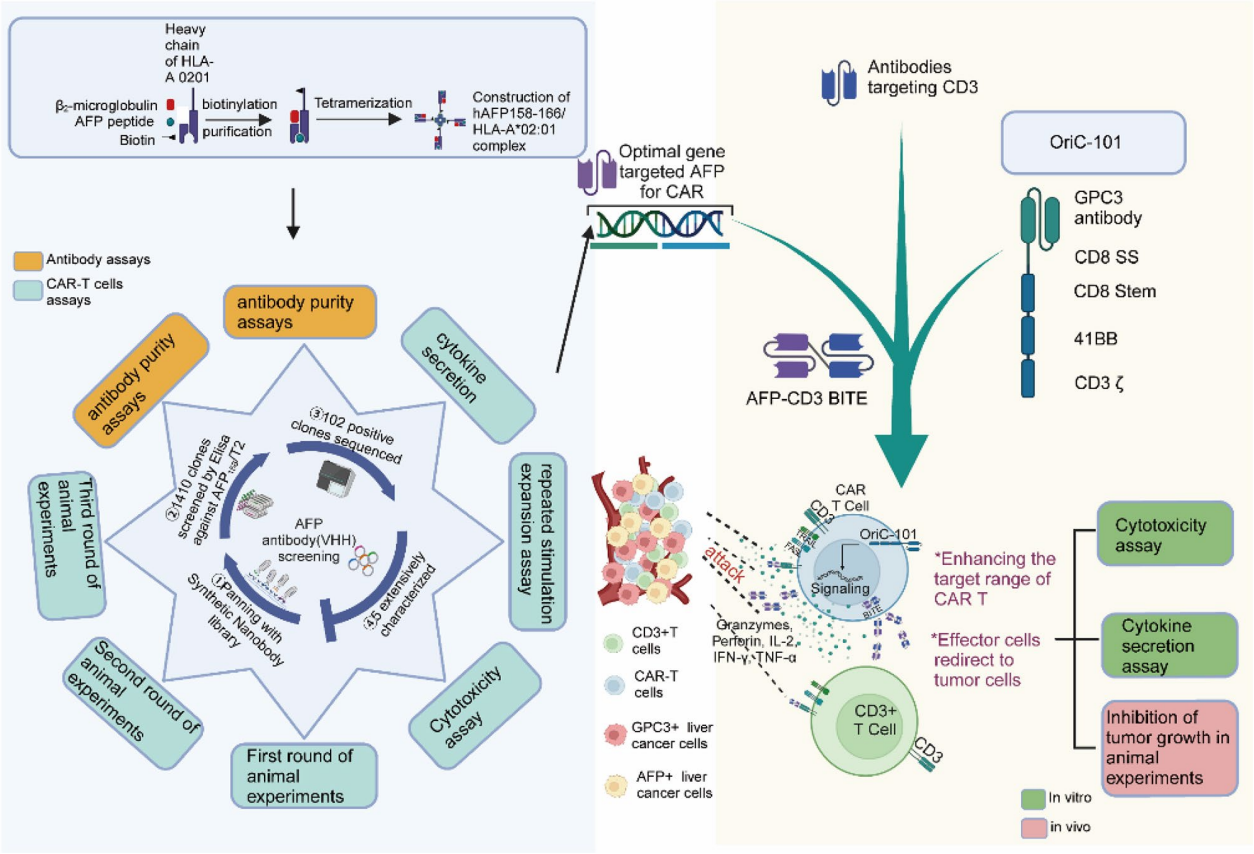

Keywords Liver cancer, Glypican-3, Alpha-fetoprotein, CAR-T, BiTE

GPC3-targeted CAR-T-cell therapy [11]. Early Phase I clinical trials have revealed promising results, with partial remission observed in 2 out of 13 patients. Notably, the median overall survival (OS) was 278 days (95% CI: 48 ~ 615 days), with favorable survival rates at 6 months, 1 year, and 3 years being 50.3%, 42.0%, and 10.5%, respectively. Moreover, the treatment demonstrated a favorable safety profile, with no significant off-target toxicities reported [12]. Excitingly, subsequent studies have shown that two patients with advanced hepatocellular carcinoma, treated with targeted GPC3 CAR-T-cell therapy along with local treatments, remained tumor-free for over seven years during long-term follow-up [13]. The investigation into GPC3-targeted CAR-T-cell therapy has become a focal point of research. Our development of a fully human anti-GPC3 antibody has shown promising outcomes in Phase I studies where 44% of patients achieved partial response, and 78% exhibited disease control [14]. Further studies revealed an overall response rate of 60%, with hepatic arterial infusion demonstrating superior efficacy compared to intravenous administration [15].

In addition to GPC3, alpha-fetoprotein(AFP) has been a crucial biomarker for liver cancer for more than 60 years [16]. It can be processed into small polypeptides that bind to HLA-A molecules, forming antigenic peptide-HLA-A complexes (pHLA-A) presented on the cell surface [17–19]. This brings a novel approach to developing CAR-T-cell therapies targeting intracellular antigens, enhancing specificity and reducing off-target toxicity [20, 21]. In safety assessments, normal cellular entities exhibited resilience to hAFP/HLA-A*02 CAR T-cell interactions, underscoring the therapy's potential [21]. Notably, the FDA has approved ET140202 CAR-T cells for treating AFP-positive advanced HCC, with patients reporting significant tumor reductions without severe adverse effects (Source: https://www.businesswire.com/news/home/20180905005262/en/Eureka-Therapeutics-Achieves-Regression-Metastatic-Liver-Cancer).

Despite these advancements, tumor heterogeneity presents a significant challenge, as liver cancer tissues

seldom exhibit uniform expression of GPC3 or AFP [22–24]. The variability within tumors limits the efficacy of CAR T-cell therapies, particularly concerning recurrence and metastasis [25]. Off-target effects may diminish the therapeutic outcomes for CAR-T cells targeting specific antigens. To address these limitations, dual-target or multi-target CAR-T-cell therapies are being explored to broaden the range of target cell antigens, potentially mitigating antigen escape and tumor recurrence. One promising strategy involvesincorporating bispecific T-cell engagers (BiTE) into CAR structures, enhancing T-cell-mediated cytotoxicity against tumor cells [26, 27]. BiTEs, comprised of two distinct single-chain variable fragments (scFv) targeting T-cell receptors and tumor-associated antigens, demonstrate improved tissue penetration and tumor cell killing efficiency while reducing off-target effects [28, 29].

This study focuses on developing CAR T-cells that target the GPC3 receptor, enhanced by the ability to secrete AFP-CD3 BiTE. This dual mechanism not only directly induces cytotoxic effects on specific targets but also has the potential to recruit and activate infiltrating $CD3^+$ T-cells in the liver tumor microenvironment, thereby synergistically enhancing anti-tumor efficacy. By integrating these innovative approaches, we aim to overcome the limitations of current therapies and improve outcomes for patients with liver cancer.

Materials and methods

Molecular synthesis of $hAFP_{158-166}$/HLA-A*02:01 complex

The pET-28a vector for prokaryotic expression was constructed by synthesizing the extracellular structural domains of human β2m and HLA-A*02:01 heavy chain molecules and splicing a BirA enzyme-dependent biotinylated sequence at the carboxyl terminus of the HLA-A*02:01 heavy chain molecule. Then, the β2m and HLA-A*02:01 proteins expressed in inclusion bodies were rinsed and primed by S200HR (chromatography column). Complexes were obtained by co-replicating with $hAFP_{158-166}$ peptide at a proportional dilution and purified by Capto Q ImpRes (a strong anion exchange medium for high-throughput media purification and fine purification). Lastly, the complex was biotin-labeled with BirA enzyme, and the biotinylated complex monomer was mixed with SAPE in a certain ratio in a gradient, and finally the two things were combined in a 4:1 ratio to form a tetramer.

Liquid phase selection

First, the AcnoviaBeads™ Streptavidin (SA beads) were conjugated with biotinylated antigen $hAFP_{158-166}$/HLA-A*02:01 and then incubated with a phage library for specific adsorption. After elution with PBST, bound phage were subsequently eluted with Gly-HCI (pH 2.2) acid wash. The eluted phage nanolibrary R1 was then mixed with a negative control peptide (hTERT540/HLA-A*02:01) to remove non-specific binding, resulting in the isolation of phages with specific binding. This selection process was repeated for a total of five rounds to achieve the enrichment of antibodies with specificity. Finally, the binding capacity between the phages and the target protein was determined using the Elisa method.

Enzyme linked immunosorbent assay (ELISA)

The Streptavidin (SA) were first conjugated with biotinylated antigen $hAFP_{158-166}$/HLA-A*02:01. Then, they were coated onto a 96-well plate overnight. 5% milk was added and sealed for 2 h, followed by 3 washes. Gradient-diluted monoclonal phages were added and allowed to bind for 1 h, followed by 3 washes. M13 secondary antibody was added and incubated for 0.5 h. Finally, TMB solution was added, and the reaction was stopped after approximately 5 min, followed by detection using an ELISA instrument.

SEC-HPLC purity analysis

The working flow rate was set to 1.0 mL/min, the pressure limit of Sepax SRT-C SEC-300 was 130 bar, the detection wavelength was 280 nm, and the column temperature was 25 °C. After column connection, rinse with ultrapure water 0.5 mL/min until the baseline is stable, followed by column equilibration at a flow rate of 1.0 mL/min for at least 5 CV until the baseline is stable, and then proceed to the sample loading operation. Pretreatment of samples: centrifuge at 10,000×g for 5 min and remove the supernatant. Gradient elution program for mobile phase: A channel. Program run time 15 min. After entering the sample information, start the injection assay. First, the buffer was added to the column, then the Protein Marker was added, and finally, the sample to be measured was added. Note that the volume of the sample to be measured should not exceed 0.5% of the column volume. The computer automatically collected data and printed the chromatogram and results, after the elution procedure.

ForteBio assays

The affinity of the antibody to the target protein was determined using ForteBio Octet RED384. Using AHC sensor, loading antibody (100nM) for 120 s. Binding peptide $hAFP_{158-166}$/HLA-A*02:01 complex (The antigen concentrations were serially diluted in a two-fold gradient starting at 150nM, resulting in seven concentrations: 150nM, 75nM, 37.5nM, 18.75nM, 9.375nM, 4.6875nM, and 0nM) for 300 s and dissociation for 400 s. Finally, the data were analyzed on the machine using Data Analysis 9.0. In this experiment, the affinity was calculated as follows: KD = koff / kon, kon: Association rate constant ($M^{-1}s^{-1}$), koff: Dissociation rate constant (s^{-1}).

KD represents the dissociation constant at equilibrium between molecular binding and dissociation (A smaller KD value indicates stronger affinity).

Identification of the specific binding activity of VHH-Fc

T2 cells with HLA-A*02:01 were loaded the human $AFP_{158-166}$ polypeptide, human TERT540 polypeptide, human NY-ESO polypeptide or other 19 human endogenous polypeptides, respectively. Among them, T2 cells loaded with human TERT540/HLA-A*02:01, human NY-ESO/HLA-A*02:01 and mixed 19 peptides were set as negative control group, and T2 cells loaded with $hAFP_{158-166}$/HLA-A*02:01 peptide fragment were set as the experimental group. The next day, different antibodies were diluted with PBS. Each antibody had an initial concentration of 10ug/ml and was diluted in a three-fold gradient, resulting in a total of seven gradients. Subsequently, 30μL of each antibody was dispensed into individual wells of a 96-well plate. Then, the 4×10^4 T2 cells loaded with different peptides were extracted and plated into each well of a 96-well plate, mixed thoroughly with antibodies, and incubated at 4°C for one hour. After the addition of secondary antibody anti-Human IgG-Fc (DyLight® 650) (abcam, UK), incubation was carried out for 30 min, followed by two washes before proceeding to machine detection.

Cell killing assay of antibodies

Human peripheral blood mononuclear cells (PBMC) were purchased from Shanghai Hycells Biotechnology Co., Ltd. (Shanghai, China) (Ethical approval number: ZJXSH-EC-C-005-AF02). The PBMC were thoroughly mixed with CD3/CD28 magnetic beads and incubated overnight in a CO2 cell culture chamber at 37 °C. At a density of 1×10^4 cells per well, they were evenly distributed in a 96-well plate. The tumor cells SK-HEP-1 ($hAFP^-$/HLA-A*0201$^+$), HepG2 ($hAFP^+$/HLA-A*0201$^-$), HepG2-MiniG ($hAFP_{158-166}{}^+$/HLA-A*0201$^+$), Raji ($hAFP^-$/HLA-A*0201$^-$), and Daudi ($hAFP^-$/HLA-A*0201$^-$) were digested and resuspended. Based on cell count results, 3×10^4 cells per well were taken and resuspended in the corresponding wells of the 96-well plate, ensuring thorough mixing of tumor cells and PBMC. Then, different antibodies were diluted in DMEM + 2%FBS culture medium to a maximum concentration of 5nM, followed by further dilution at a 10-fold ratio to establish three concentration gradients. They were added to the corresponding wells of the 96-well plate and thoroughly mixed with tumor cells and PBMC. The aforementioned plate was incubated at 37 °C in a 5% CO2 incubator for 20 h. Lysis buffer was added to the wells, followed by continued incubation in the original incubator for 45 min. Finally, the supernatant was transferred to an enzyme analysis plate, and reaction substrates and stop solution were sequentially added. The absorbance was measured and read at OD_{490}.

Targeted cell line construction

The plasmid packaging virus was used to package the lentivirus expressing $hAFP_{158-166}$. Subsequently, SK-HEP-1 and HepG2 cell lines were infected with the virus. After flow cytometry sorting, monoclonal clones were obtained. The expression of $hAFP_{158-166}$ in the cell lines was identified through flow cytometry analysis after expansion in culture. The identified cell lines were named SK-HEP-1-MiniG and HepG2-MiniG, respectively.

The same method was employed to construct plasmids overexpressing GPC3 and $hAFP_{158-166}$, which were then packaged into lentivirus and used to infect SK-HEP-1 cell line. After flow cytometry sorting, monoclonal clones were obtained. The expression of GPC3 and $hAFP_{158-166}$ in the cell lines was identified through flow cytometry analysis after expansion in culture. The identified cell lines were named SK-HEP-1-GPC3-AFP.

CAR-T cell construction

Preparation of Reagents for T cell sorting

Buffer 1: Prepare by diluting 20% HSA (Human Serum Albumin) with 0.9% NaCl at a 1:9 ratio.

Buffer 2: 97.1% PBS (v/v) + 2.5% 20% HSA (v/v) + 0.4% 0.5 M EDTA (v/v).

Buffer 3: Pre-chill Buffer 2 at 4 °C.

X-VIVO Complete Medium: X-VIVO + 5% FBS + IL-7 (10 ng/mL final concentration) + IL-21 (20 ng/mL final concentration).

Experimental procedure: Thaw one vial of PBMCs in a 37 °C water bath. Add 10× volume of Buffer 1 to the PBMCs, then centrifuge at 500 g for 5 min at room temperature. Discard the supernatant. Resuspend the cells in 10 ml Buffer (1) Take 20 μl for cell counting. Based on the result of cell count, add 80 μl Buffer 3 and 20 μl CD3 MicroBeads (CD3 MicroBeads, human - lyophilized, Miltenyi Biotec) per 1×10^7 cells. Incubate at 4 °C for 15 min. After incubation, add 1.5 ml Buffer 3 per 1×10^7 cells to wash. Resuspend PBMCs in an appropriate volume of Buffer (2) Isolate $CD3^+$ T cells using a MACS separator and LS column. Rinse both the PBMCs and the column with Buffer 2. After separation, apply positive pressure with the plunger to elute the liquid from the column and collect $CD3^+$ cells. Resuspend the collected $CD3^+$ cells in X-VIVO complete medium and count. Adjust the cell density to 1.25×10^6 cells/ml. Add CD3/CD28 beads at a 3:1 bead-to-cell ratio based on the cell count. Transfer to a 37 °C incubator for culture. On the following day, add CAR-containing viral supernatant to the isolated $CD3^+$ T cells at an MOI of 4. Mix gently and return to the 37 °C incubator. After 18–24 h, remove the viral supernatant by centrifugation and continue

culturing at 37 °C. On day 5, remove CD3/CD28 beads using a magnetic stand. Supplement with fresh X-VIVO complete medium and continue culture. Between days 7–12, perform quality control on the expanded cells, which are then ready for subsequent in vitro and in vivo experiments.

CAR-T cell cytotoxicity and cytokine detection

On the 7th day of CAR-T cell culture, the flow cytometry was performed to detect the positivity rate of CAR-T cells. Based on the results of the positivity rate, an equal number of CAR-T cells were selected using the lowest positivity rate as the criterion. Mock T cells were used for adjustment to ensure an equal total cell count in each group. Target cells were digested, resuspended, and counted. Then, they were plated in a 96-well plate at a density of 1×10^4 cells per well. The effector-to-target ratio was set at 1:1, and CAR-T cells were added and thoroughly mixed. The plate was incubated at 37 °C for a total of 20 h. After incubation, 50μL of the suspension was taken and added to a 96-well enzyme detection plate. Subsequently, according to the instructions of the LDH detection kit (Promega, USA), the substrate and stop solution from the LDH kit were added in sequence, and the absorbance was read at OD = 490 nm using an ELISA reader (Bio Tek, USA).

The Capture from the IL2 and IFN-γ assay kits (R&D Systems, USA) were added to a 96-well ELISA plate and stored overnight at 4 °C. The plate was washed three times with 0.05% PBST buffer, and then the milk blocking solution was added at room temperature for blocking. The standard samples from the IL2 and IFN-γ assay kits were diluted. Meanwhile, 100μL of the supernatant from the PBMC and CAR-T cell suspension, obtained after centrifugation, was taken and added to the 96-well ELISA plate. The supernatant and standard samples were incubated at room temperature for 2 h. After washing, the diluted Detect solution, diluted Streptavidin-HRP (R&D Systems, USA), TMB solution (Invitrogen™, USA), and stop solution (Solarbio, China) were added sequentially according to the instructions. Finally, the absorbance was read at OD = 450 nm using an ELISA reader.

CAR-T cell repetitive stimulation experiment

The positivity rate of CAR-T cells cultured on day 9 was determined by flow cytometry. Based on the results of the positivity rate, an equal number of CAR-T cells was selected using the lowest positivity rate as the criterion. Mock T cells were adjusted to ensure an equal total cell count in each group. Target cells were digested, resuspended, and counted. They were then plated in a 12-well plate at a density of 1×10^5 cells per well for the first round of stimulation, with an effector-to-target ratio set at 1:1. Subsequently, target cells and effector cells were mixed and resuspended in X-VIVO medium for plating in a 12-well plate. The plates were incubated together in a 37℃ incubator for approximately 3 days. Cell counting was initiated, and for the second round of stimulation, the amount of target cells was calculated based on the CAR-T cell count and positivity rate obtained after the first round of stimulation.

Analysis of the parameterized transcriptome sequencing of CAR-T cells

In an effort to gain a superior understanding of the distinctions between BiTE-structured CAR-T and other control group CAR-T, we have conducted an experiment of reference-based transcriptome sequencing analysis. his experiment was entrusted to Shanghai OE Biotech Co., Ltd. to accomplish, and its online data analysis platform (OE Cloud Platform) was utilized to complete part of the data analysis and image plotting. After obtaining the differential genes, we set the conditions ($P < 0.05$ and $|\log_2^{\text{fold change}}| \geq 4$), and further carried out the screening of differential genes. The differential genes thus obtained were employed to plot the PPI network and the screening of Hub genes. Conduct GO and KEGG Pathway enrichment analysis of differential genes via the OECloud platform and graphically represent it.

Flow cytometric analysis of memory CAR-T cell functional subsets

CAR-T cell functional subpopulations were identified before and after repeated stimulation of CAR-T cells. Flow cytometry was employed to detect the expression of surface markers on CAR-T cells, in order to determine the proportions of different functional subpopulations. The identification of functional subpopulations was performed using specific antibodies: BV510 Mouse Anti-Human CD45RO (BD, USA), PE Rat Anti-Human CCR7 (BD, USA), FITC Mouse Anti-Human CD3 (BD, USA), Myc-Tag (9B11) Mouse mAb (Alexa Fluor® 647 Conjugate) (CST, USA). Each group of CAR-T cells was stained at 4 °C for 0.5-1 h, washed with PBS, and resuspended for machine detection.

Mouse xenograft tumor model and CAR-T treatment

Female B-NDG mice (Biocytogen, China) were inoculated with human-derived hepatocellular carcinoma cells SK-HEP-1-MiniG ($hAFP_{158\text{-}166}^{+}$/HLA-A*02:01^{+}) under the right axilla to establish a subcutaneous xenograft tumor model in SK-HEP-1-MiniG B-NDG mice (Ethical Approval for Animal Experimentation No. YS-m202306002). After inoculation, the tumor-bearing mice were grouped according to the tumor volume using the randomized grouping method. CAR-T cells were injected intratumorally or into the tail vein. Animals were monitored continuously for weight and tumor volume,

and euthanized when their health status continued to deteriorate or when body weight was reduced by more than 20%.

Results

Expression analysis of AFP and GPC3 in liver cancer

To develop effective and safe CAR-T cell therapy for liver cancer, we investigated the expression of AFP and GPC3 in hepatocellular carcinoma (HCC) and normal tissues. This analysis helps predict potential therapeutic effects and adverse events associated with CAR-T products targeting these antigens.

We utilized the GEPIA2 database (http://gepia2.cancer-pku.cn), which includes gene expression data from The Cancer Genome Atlas (TCGA). Analysis of pan-cancer samples revealed significant expression of AFP and GPC3 primarily in liver cancer tissues, with minimal expression in normal tissues and other cancer types (Supplementary Fig. 1A, B and Supplementary Tables 1, 2).

Furthermore, we analyzed a cohort of 368 tumor tissues and 160 normal liver tissues from patients with HCC. This analysis confirmed significant differences in the expression levels of AFP and GPC3 between liver cancer tissue and adjacent non-cancerous tissues (Supplementary Fig. 1C and D).

To strengthen the clinical relevance of our findings, we conducted a retrospective analysis on 65 liver cancer patients diagnosed between 2014 and 2021 at Zhuhai People's Hospital. Immunohistochemical staining of their pathological specimens revealed that 50.77% of the patients were positive for AFP, 70.77% were positive for GPC3, and 38.46% expressed both antigens (Supplementary Fig. 1E, F, G and Supplementary Table 3).

These findings strongly suggest that CAR-T cells targeting AFP and GPC3, liver cancer-specific antigens, hold promise for improved treatment efficacy and enhanced safety.

Development of high-affinity AFP-specific antibody

Building on the success of our second-generation GPC3 CAR-T with high anti-tumor efficacy, we are initiating the development of an AFP-targeting TCR mimic antibody to explore potential synergistic effects in combination therapy.

Given the high prevalence of the HLA-A*02:01 allele (8.15% globally, 12.04% in China), we focused on constructing the $hAFP_{158-166}$/HLA-A*02:01 complex for optimal antigen presentation (Fig. 1A Up). Following purification of recombinantβ2m and HLA-A*02:01 proteins, we co-complexed them with the $hAFP_{158-166}$ peptide at a defined ratio. Utilizing Capto Q ImpRes, we purified the complexes to achieve 99.09% purity (Fig. 1A Down).

To identify high-affinity antibodies targeting AFP presented by HLA-A*02:01, we employed a biopanning strategy on an artificially synthesized phage display antibody library. After five rounds of liquid-phase screening, we identified five candidate VHH antibodies (Fig. 1B, C, D). Monoclonal ELISA was used to select five candidate antibodies exhibiting low background and significant signal-to-noise ratios. These candidates were sequenced and designated as 1B3, 1C11, 1C4, 1D12, and 2F9. Notably, the Ab61 antibody, encoded by the gene described in patent CN107106671A, was synthesized as a positive control. Protein A affinity chromatography purified this positive control. Subsequent one-step Protein A affinity chromatography and SEC-HPLC analysis confirmed high purity for all VHH antibodies (Supplementary Fig. 2A, B and Supplementary Table 4).

Finally, affinity assays were performed using a ForteBio AHC sensor-conjugated antibody loaded with each candidate antibody and the $hAFP_{158-166}$/HLA-A*02:01 complex. All candidate antibodies, except 1D12, demonstrated superior dissociation constants compared to the Ab61 positive control. Notably, the 1B3 antibody exhibited an affinity constant approximately five-fold higher than Ab61 (Fig. 1E and Supplementary Table 5).

These results highlight the successful development of a high-affinity, specific antibody (1B3) targeting hAFP presented by HLA-A*02:01, a crucial component for our dual-targeting CAR-T cell therapy strategy.

In vitro functional evaluation of the VHH antibodies for AFP and the associated CAR-T

To assess the specificity of the VHH antibodies, we performed binding assays using T2 cells (The T2 Cell is a human lymphocyte hybridoma cell that faithfully presents the target antigenic peptide to the cell surface, thereby targeting the T cell corresponding to the target antibody.), loaded with various peptide antigens. The results demonstrated that the antibodies exhibited high specificity for the $hAFP_{158-166}$/HLA-A*02:01 complex, with minimal binding to T2 cells loaded with irrelevant peptides (Fig. 2A). Notably, the 1B3 antibody demonstrated strong binding affinity not only to the HLA-A*02:01 complex but also to the HLA-A*02:07 complex, suggesting potential applicability in a broader patient population (Supplementary Fig. 2C and D).

To evaluate the cytotoxic potential of the VHH antibodies, we conducted in vitro ADCC assays. The target cells (HepG2) were engineered to express the hAFP158-166/HLA-A*02:01 complex on their surface (HepG2-MiniG). We co-cultured various tumor cell lines HepG2 cell ($hAFP^+$/HLA-A*02:01$^-$), HepG2-MiniG cell ($hAFP_{158-166}{}^+$/HLA-A*02:01$^+$), SK-HEP-1 cell ($hAFP^-$/HLA-A*02:01$^+$), and Raji cell ($hAFP^-$/HLA-A*02:01$^-$) and Daudi cell ($hAFP^-$/HLA-A*02:01$^-$) with PBMCs

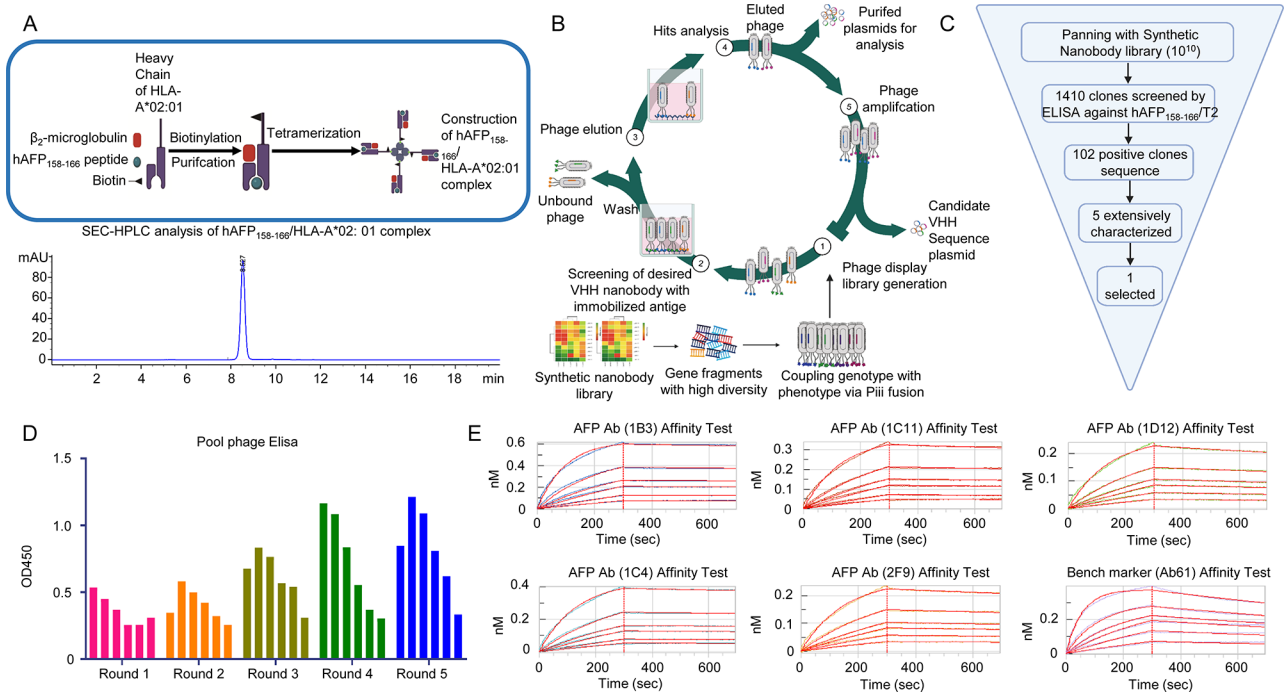

Fig. 1 (**A**) Up, Construction process of $hAFP_{158\text{-}166}$/HLA-A*02:01 complex. Down, Purity analysis of $hAFP_{158\text{-}166}$/HLA-A*02:01 complex by SEC-HPLC. (**B**) Antibody screening process: ① Synthesis of artificial nanobody phage display library. ② Screening for humanized VHH antibodies. ③ Elution of phages. ④ Analysis of target phages. ⑤ Phage amplification and acquisition of candidate VHH plasmid sequences. (**C**) The acquisition and screening process of antibodies. (**D**) Five rounds of liquid phase elution antibody enrichment effect (In each round of elution, each column represents a concentration gradient of phage stock solution, which is diluted into a gradient at a 3-fold ratio from left to right). (**E**) Results of affinity assay of different antibodies binding to peptide $hAFP_{158\text{-}166}$/HLA-A*02:01: the affinity of AFP Ab (1B3) antibody reached 0.504nM; the affinity of AFP Ab (1C11) antibody was 1.21nM; the affinity of AFP Ab (1D12) antibody was 3.02nM; the affinity of AFP Ab (1C4) was 0.865nM; the affinity of AFP Ab (2F9) was 2.06nM; the affinity of Bench marker (Ab61) was 2.34nM. The affinity of the three antibodies (1C11, 1D12 and 2F9) was comparable to the Bench marker (Ab61) (The six curves in Figure E are the fitted curves for the first six antigen concentrations)

and different VHH antibodies. The results showed that all five antibodies exhibited specific cytotoxicity against $hAFP_{158-166}{}^{+}$/HLA-A*02:01^{+} tumor cells, with minimal non-specific killing of other cell lines (Supplementary Fig. 3A, B, C, D and E). It is particularly noteworthy that the AFP Ab (1B3) and AFP Ab (1C11) antibodies did not exhibit non-specific cytotoxicity against SK-HEP-1 cells at any concentration (Supplementary Fig. 3D).

To further investigate the therapeutic potential of these VHH antibodies, we engineered CAR-T cells incorporating the VHH sequences. The target cells (SK-HEP-1 and HepG2) were engineered to express the $hAFP_{158-166}$/HLA-A*02:01 complex on their surface (named SK-HEP-1-MiniG and HepG2-MiniG), enabling recognition and elimination by CAR-T cells (Fig. 2B).

In vitro repeated stimulation experiments demonstrated that 1B3 CAR-T cells exhibited robust expansion and specific cytotoxicity against target cells, comparable to the positive control Ab61 CAR-T cells. Moreover, 1B3 CAR-T cells displayed lower non-specific cytotoxicity against hAFP^{-}/HLA-A*02:01^{-} cells, suggesting improved safety. Cytokine release assays revealed that 1B3 CAR-T cells produced similar levels of cytotoxic cytokines as Ab61 CAR-T cells, but with lower baseline cytokine secretion in the absence of target cells. This suggests that 1B3 CAR-T cells may offer a favorable balance of efficacy and safety (Fig. 2C, D, E, and F).

These findings collectively demonstrate the promising potential of the AFP Ab (1B3) antibody and its corresponding CAR-T cells for the targeted treatment of liver cancer, particularly in patients expressing HLA-A*02:01 or HLA-A*02:07.

In vivo efficacy of 1B3 CAR-T cells

To evaluate the in vivo efficacy of 1B3 CAR-T cells, we established a subcutaneous tumor model using SK-HEP-1-MiniG cells in mice. Treatment with 1B3 CAR-T cells significantly inhibited tumor growth compared to the control group (Fig. 3A, B, and C). Notably, intratumoral administration of CAR-T cells demonstrated enhanced efficacy compared to intravenous administration. Importantly, 1B3 CAR-T cells were well-tolerated, with no significant changes in body weight observed (Fig. 3D).

To further assess the durability of the anti-tumor response, we established a secondary tumor challenge model (Fig. 4A and Supplementary Table 6). Mice were

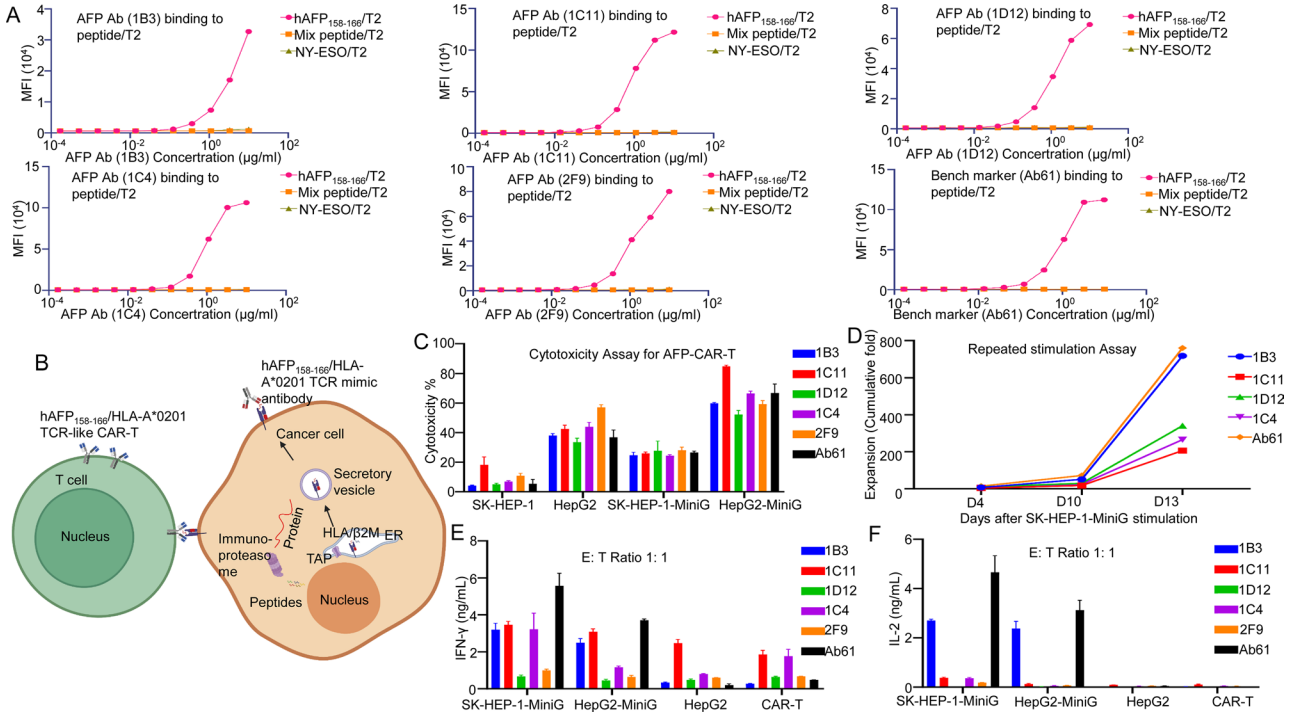

Fig. 2 (**A**) All antibodies showed binding activity to T2 cells loaded with $hAFP_{158-166}$ peptide, but had non-specific binding to T2 cells loaded with NY-ESO and 19 mixed peptides. (**B**) Illustration of $hAFP_{158-166}$/HLA-A*02:01 TCR-like CAR-T binding to tumor cells and killing them. (**C**) In vitro cytotoxicity assay of CAR-T cells constructed with various antibodies against different cancer cells (SK-HEP-1, HepG2, SK-HEP-1-MiniG, HepG2-MiniG). (**D**) The fold expansion of each CAR-T cell in the in vitro repeated stimulation experiment (target cells: SK-HEP-1-MiniG). (**E**) The secretion levels of IFN-γ by CAR-T cells in the cytotoxicity assay at an effector-to-target ratio of 1:1. (**F**) The secretion levels of IL-2 by CAR-T cells in the cytotoxicity experiment at an effector-to-target ratio of 1:1

treated with 1B3 CAR-T cells and, after complete tumor regression, were re-challenged with SK-HEP-1-MiniG cells on the contralateral flank. Remarkably, even at lower doses, 1B3 CAR-T cells effectively inhibited the growth of the secondary tumor, demonstrating potent long-lasting anti-tumor activity (Fig. 4B).

To investigate the mechanisms underlying the therapeutic efficacy of 1B3 CAR-T cells, we analyzed the persistence and cytokine release profiles of these cells in vivo. Flow cytometry analysis revealed that 1B3 CAR-T cells persisted in the tumor microenvironment for an extended period, contributing to sustained tumor control (Fig. 4C). Additionally, 1B3 CAR-T cells exhibited a balanced cytokine release profile, with elevated levels of IFN-γ and IL-2, crucial for effective tumor cell killing and T cell proliferation, respectively (Fig. 4D, E).

The safety profile of 1B3 CAR-T cells was assessed by monitoring body weight and peripheral cytokine levels. No significant weight loss was observed in any of the treatment groups, indicating good tolerability (Supplementary Fig. 4A). Notably, 1B3 CAR-T cells induced lower levels of IL-6, a cytokine associated with cytokine release syndrome (CRS), compared to the Ab61 control (Supplementary Fig. 4B). These findings suggest that 1B3 CAR-T cells may have a favorable safety profile, with a reduced risk of cytokine release syndrome.

Low-dose 1B3 CAR-T therapy: a promising approach for cancer treatment

To further investigate the therapeutic potential of 1B3 CAR-T cells, we conducted a third round of in vivo experiments, focusing on low-dose therapy. Mice bearing subcutaneous SK-HEP-1- MiniG tumors were treated with intratumoral injections of 1×10^6 or 3×10^5 1B3 or Ab61 CAR-T cells (Fig. 5A). Remarkably, even at the low dose of 3×10^5 cells, 1B3 CAR-T cells demonstrated superior tumor suppression compared to Ab61 CAR-T cells (Fig. 5B and Supplementary Table 7). To assess the long-term efficacy, mice were re-challenged with tumor cells on the contralateral flank. Both 1B3 and Ab61 CAR-T cells effectively suppressed tumor recurrence, highlighting the durability of the anti-tumor response (Fig. 5B).

In contrast to the previous experiments with higher initial tumor burden and CAR-T cell doses, the peak in CAR-T cell expansion and cytokine release occurred later in the low-dose setting. Specifically, a peak in IFN-γ and TNF-α levels was observed on day 14, while IL-2 levels remained elevated throughout the study period (Fig. 5C, D, E and Supplementary Fig. 4D).

Regarding safety, no significant weight loss was observed in any treatment group (Supplementary Fig. 4C). The transient elevation in IL-6 levels, a cytokine associated with cytokine release syndrome (CRS), was

A

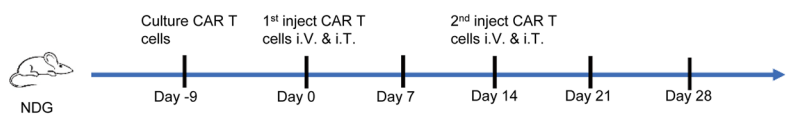

B

Serial	Group	Number	Dose	Method	Mean of tumor volume on D59 (mm^3)	Number of tumor-free animals on D59	Tumor growth inhibition rate on D59
G1	Mock-T	5	1E7 cells	I.V. Day 0	1194.87/211.66	-	0
G2	Ab61 CAR-T	5	1E7 cells	I.T. Day 0, Day14	0/0	5	107.99%
G3	1B3 CAR-T	5	1E7 cells	I.T. Day0, Day14	0/0	5	107.96%
G4	Ab61 CAR-T	5	1E7 cells	I.V. Day0	10.49/1.27	-	107.04%
G5	1B3 CAR-T	5	1E7 cells	I.V. Day0	16.04/2.45	-	106.55%

Note: I.V., tail vein injection. I.T., intratumoral injection.

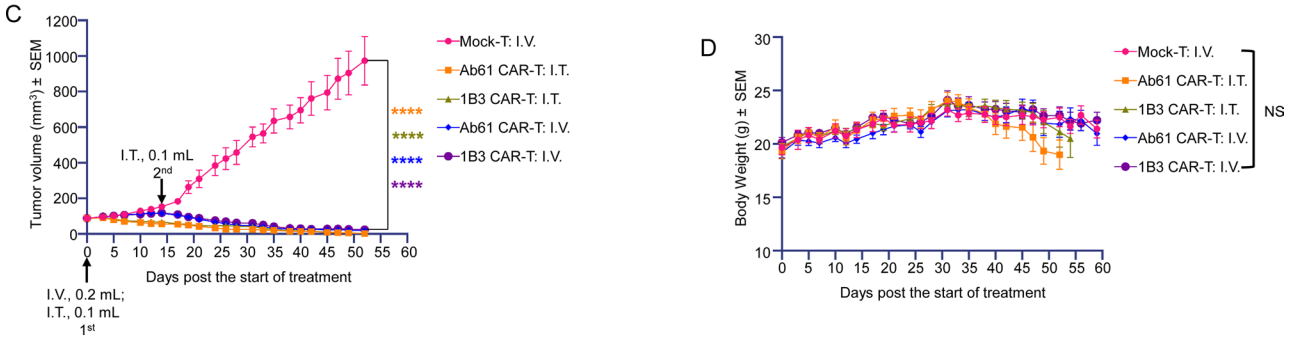

Fig. 3 (**A**) Flow chart of the first round animal experiments (In this study, the first CAR-T cell therapy injection was administered on Day 0, SK-HEP-1-MiniG were inoculated in mice on Day −9, and the second CAR-T cell therapy injection was administered on Day 14. Throughout the experimental period, tumor size was measured three times per week. The proportion of human T cells and cytokine levels were assessed through peripheral blood testing). (**B**) Administration methods and dosages of CAR-T in each group, tumor volume of mice at endpoint, and tumor inhibition rate. (**C**) Tumor growth curve of mice in all groups (each group: $n = 5$). (**D**) Changes in body weight of mice in each treatment group (each group: $n = 5$)

minimal and did not persist. These findings suggest that low-dose 1B3 CAR-T therapy offers a favorable safety profile with minimal adverse effects.

Overall, these results demonstrate the potent anti-tumor activity and favorable safety profile of low-dose 1B3 CAR-T therapy. This approach holds significant promise for the treatment of liver cancer with 1B3 antibody targeting AFP.

GPC3 CAR-T cells with integrated AFP-CD3 bite: enhanced anti-tumor activity

While our previous generation of GPC3 CAR-T cells demonstrated promising anti-tumor activity, we sought to further optimize their efficacy by incorporating additional targeting strategies. The integration of an optimized AFP-CD3 BiTE into the CAR-T cell design provides a dual-targeting approach, potentially enhancing tumor cell killing and overcoming potential resistance mechanisms.

We constructed second-generation GPC3 CAR-T cells incorporating 4-1BB as a co-stimulatory domain, integrated an optimized, secreted AFP-CD3 BiTE into the CAR-T cell design. The BiTE molecule, upon secretion, can bind to both AFP-expressing tumor cells and T cells, both endogenous and CAR-T cells, forming an immune synapse and activating bystander T cells (Fig. 6A, B).

To evaluate the functional activity of these CAR-T cells, we established a target cell line (Sk-hep-1-GPC3-AFP) overexpressing both GPC3 and the $hAFP_{158-166}$/HLA-A*02:01 complex (Fig. 6C). In vitro cytotoxicity assays and repeated stimulation experiments demonstrated that GPC3 CAR-T cells with the integrated AFP-CD3 BiTE (GPC3 CAR-T-AFP-CD3) exhibited superior anti-tumor activity compared to single-target GPC3 CAR-T cells (Fig. 6F, G). Furthermore, phenotypic analysis revealed that GPC3 CAR-T-AFP-CD3 cells displayed a mixed phenotype of central memory T cells (T_{CM}) and effector memory T cells (T_{EM}) (Fig. 6D, E). This suggests that GPC3 CAR-T-AFP-CD3 cells may possess enhanced persistence and long-term anti-tumor activity. Notably, GPC3 CAR-T-AFP-CD3 cells consistently demonstrated superior performance in both cytotoxicity assays and IFN-γ secretion assays (Fig. 6F, G).

These findings highlight the potential of our dual-targeting strategy to improve the efficacy of CAR-T cell therapy for liver cancer. By combining direct tumor cell killing with bystander T cell activation, this approach may overcome the challenges associated with tumor heterogeneity and immune suppression.

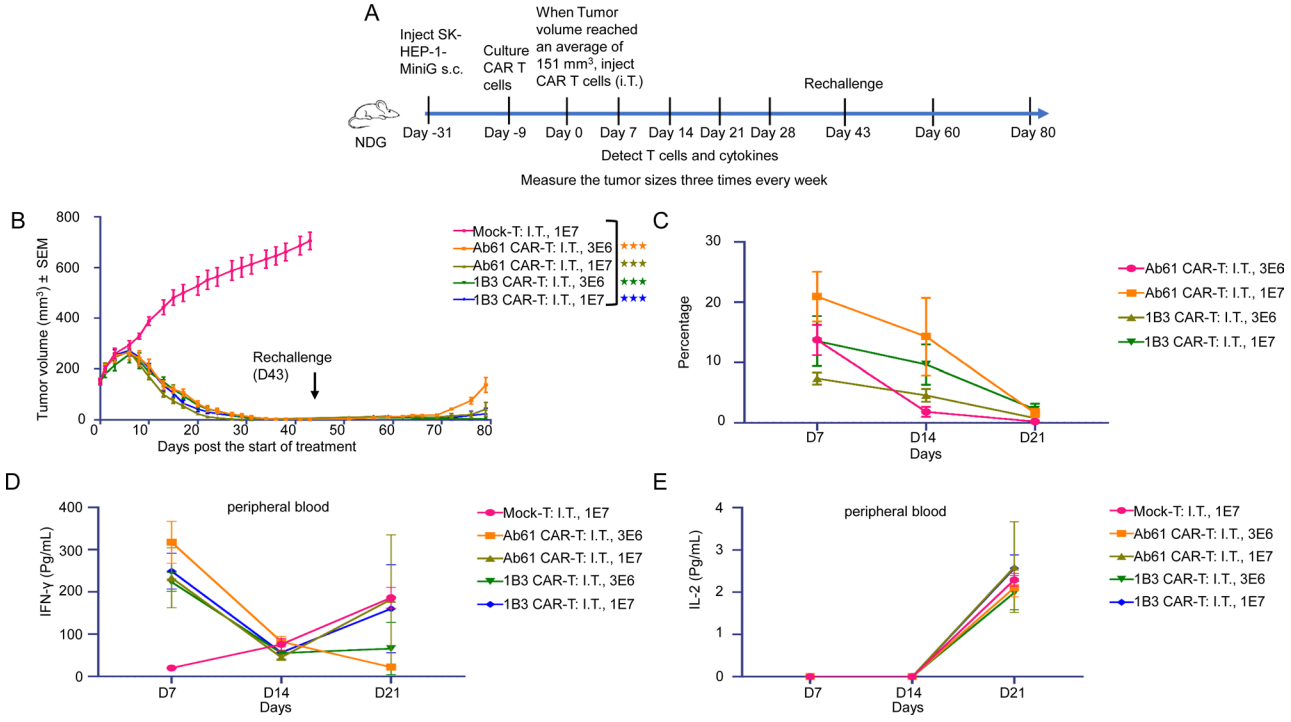

Fig. 4 (**A**) Flow chart of the second round animal experiments (In this study, SK-HEP-1-MiniG cells were inoculated subcutaneously in the right flank of mice on Day − 31. When the average tumor volume reached 151 mm^3, CAR-T cells were administered via intratumoral injection. Due to significant tumor regression, tumor cells were re-inoculated subcutaneously in the left flank on Day 43 to simulate a tumor recurrence model, aiming to evaluate the sustained anti-tumor efficacy of CAR-T cells). (**B**) Tumor growth curve of mice in all groups, rechallenge: mice with tumor regression were rechallenged with tumor cells on the contralateral side to observe the long-lasting tumor-suppressive effects of CAR-T (each group: $n = 5$). (**C**) CAR-positive rate of CAR-T cells in peripheral blood of mice on day 7, day 14 and day 21 (each group: $n = 5$). (**D**) Secretion level of IFN-γ in the peripheral blood serum of mice on day 7, day 14 and day 21 (each group: $n = 5$). (**E**) Secretion level of IL-2 in the peripheral blood serum of mice on day 7, day 14 and day 21 (each group: $n = 5$)

Mechanistic insights into enhanced efficacy of GPC3 CAR-T-AFP-CD3 cells

To understand the mechanisms underlying the superior anti-tumor activity of GPC3 CAR-T-AFP-CD3 cells, we performed transcriptome sequencing on these cells after repeated stimulation. Principal component analysis revealed distinct gene expression profiles between GPC3 CAR-T-AFP-CD3 cells and control groups (Fig. 7A and B). Volcano plots and Venn diagrams identified differentially expressed genes (DEGs) across groups (Figs. 7C-F and Supplementary Tables 8, 9, 10 and 11). Gene Ontology (GO) and Kyoto Encyclopedia of Genes and Genomes (KEGG) pathway analyses revealed enrichment of pathways associated with enhanced T cell function in GPC3 CAR-T-AFP-CD3 cells compared to controls (Supplementary Fig. 5A, B, C, D, E and F). Notably, genes like TNF, CD40LG, and CSF2 emerged as key players in the functional distinction between GPC3 CAR-T-AFP-CD3 and other CAR-T cell variants (Fig. 7G, H and I). These findings suggest that the incorporation of the AFP-CD3 BiTE into GPC3 CAR-T cells (GPC3 CAR-T-AFP-CD3) modulates gene expression, potentially contributing to their superior anti-tumor activity. Further investigation of these key genes may provide valuable insights for optimizing CAR-T cell therapy for liver cancer.

In vivo efficacy of GPC3 CAR-T with AFP-CD3 bite

To assess the in vivo efficacy of GPC3 CAR-T cells with the integrated AFP-CD3 BiTE (GPC3 CAR-T-AFP-CD3), we established a subcutaneous tumor model in mice (Fig. 8A). When tumor volumes reached 80–120 mm^3, mice were intravenously administered with 1×10^6 or 3×10^6 CAR-T cells. The group treated with 3×10^6 GPC3 CAR-T-AFP-CD3 cells exhibited significant tumor growth inhibition and prolonged survival compared to the control groups (Fig. 8B and Supplementary Table 12). Importantly, no significant weight loss was observed in any treatment group, indicating a favorable safety profile (Fig. 8C). Furthermore, increased levels of IFN-γ in the peripheral blood and expansion of CAR-positive T cells were observed in mice treated with GPC3 CAR-T-AFP-CD3 cells (Fig. 8D, E). These findings suggest that the BiTE-based strategy enhances the anti-tumor activity of CAR-T cells, with the potential recruiting and activating endogenous T cells.

In conclusion, our study demonstrates the potential of GPC3 CAR-T cells with the integrated AFP-CD3 BiTE as

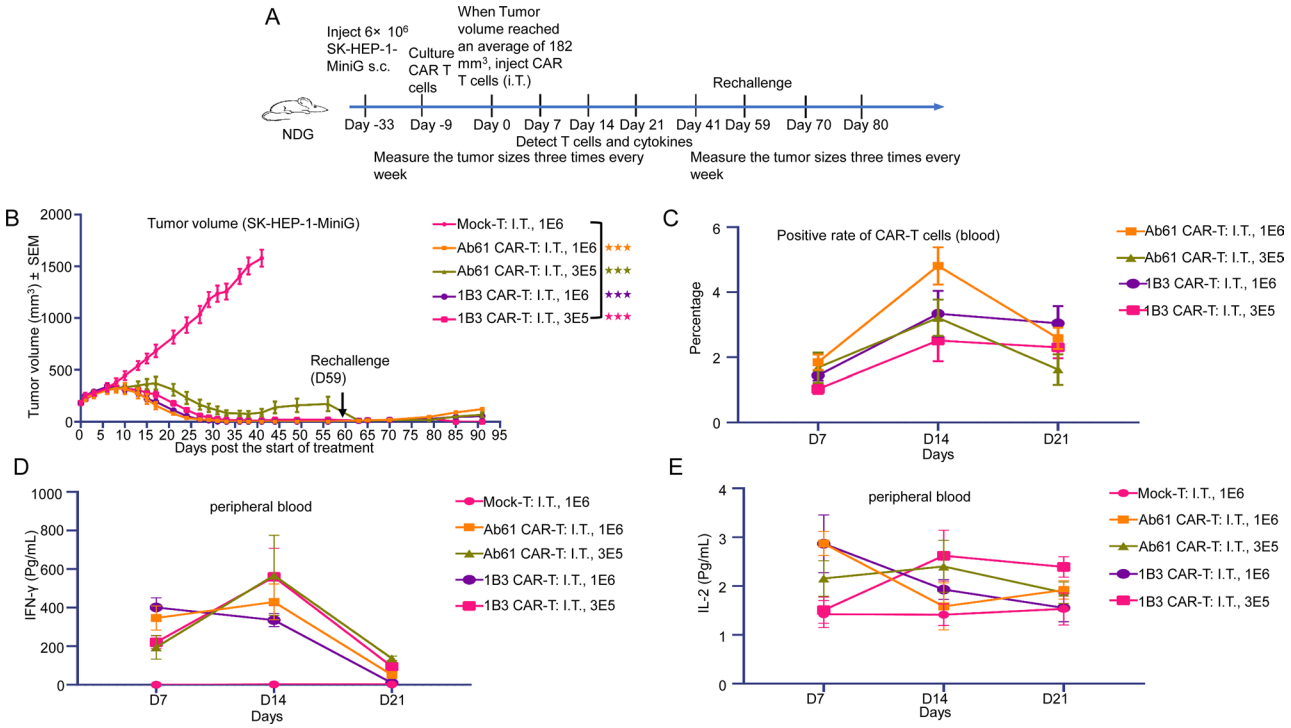

Fig. 5 (**A**) Flow chart of the third round animal experiments (In this experiment, to challenge CAR-T cells with larger tumors, we inoculated SK-HEP-1-MiniG cells subcutaneously on the right flank of mice on Day −33. When the tumor volume reached 182 mm^3, CAR-T cells were administered via intratumoral injection. Subsequently, rapid tumor regression was observed. On Day 59, mice were re-challenged with SK-HEP-1-MiniG cells subcutaneously on the left flank to assess the long-term antitumor efficacy of CAR-T cells). (**B**) Tumor growth curve of mice in all groups, rechallenge: mice with tumor regression were rechallenged with tumor cells on the contralateral side to observe the long-lasting tumor-suppressive effects of CAR-T (each group: $n=5$). (**C**) CAR-positive rate of CAR-T cells in peripheral blood of mice on day 7, day 14 and day 21 (each group: $n=5$). (**D**) Secretion level of IFN-γ in the peripheral blood serum of mice on day 7, day 14 and day 21 (each group: $n=5$). (**E**) Secretion level of IL-2 in the peripheral blood serum of mice on day 7, day 14 and day 21 (each group: $n=5$)

a promising therapeutic approach for liver cancer. This dual-targeting strategy offers improved anti-tumor efficacy and a favorable safety profile, making it a promising candidate for future clinical translation.

Discussion

CAR-T cell therapy has emerged as a revolutionary treatment for hematologic malignancies, achieving remarkable success by harnessing the power of a patient's own immune system [30]. However, its application to solid tumors, like liver cancer, presents a unique challenge. Unlike blood cancers with well-defined antigens, solid tumors exhibit a complex and heterogeneous microenvironment [31]. Additionally, the scarcity of tumor-specific antigens further complicates the development of effective CAR-T therapies [32–34].

In this study, we first screened the antibody IB3 with high affinity for targeting the AFP target. During in vitro experiments, we validated the killing efficacy of the antibody and its constructed CAR-T cells, and observed that when the direct killing effect was robust, CAR-T cells directly acted on tumor cells, inducing their apoptosis or cell death, while secreting relatively lower levels of cytokines such as IL-2 and IFN-γ (Fig. 2C). In animal model validation, we demonstrated that when higher CAR-T cell dosage coincided with lower tumor burden, mirroring observations from in vitro experiments, the enhanced direct cytotoxic activity of CAR-T cells led to correspondingly reduced levels of cytokine secretion (Figs. 4, 5 and 8). This phenomenon has been similarly reported in previous literature [35].

This study presents a novel approach to tackling these challenges by introducing a dual-targeting CAR-T cell therapy strategy for liver cancer. Our approach focuses on two key antigens: alpha-fetoprotein (AFP) and GPC3. AFP is an intracellular protein often elevated in liver cancer patients, and can be presented by specific HLA to cancer cell surface as TCR and TCR mimic antibody target, while GPC3 is a cell surface antigen highly expressed on liver cancer cells. By targeting both antigens, we aim to achieve broader patient applicability and enhanced anti-tumor efficacy.

To enhance the efficacy of CAR-T cell therapy in liver cancer, we incorporated a dual-targeting strategy by combining GPC3 CAR-T cells with an optimized AFP-CD3 BiTE structure. This innovative approach leverages

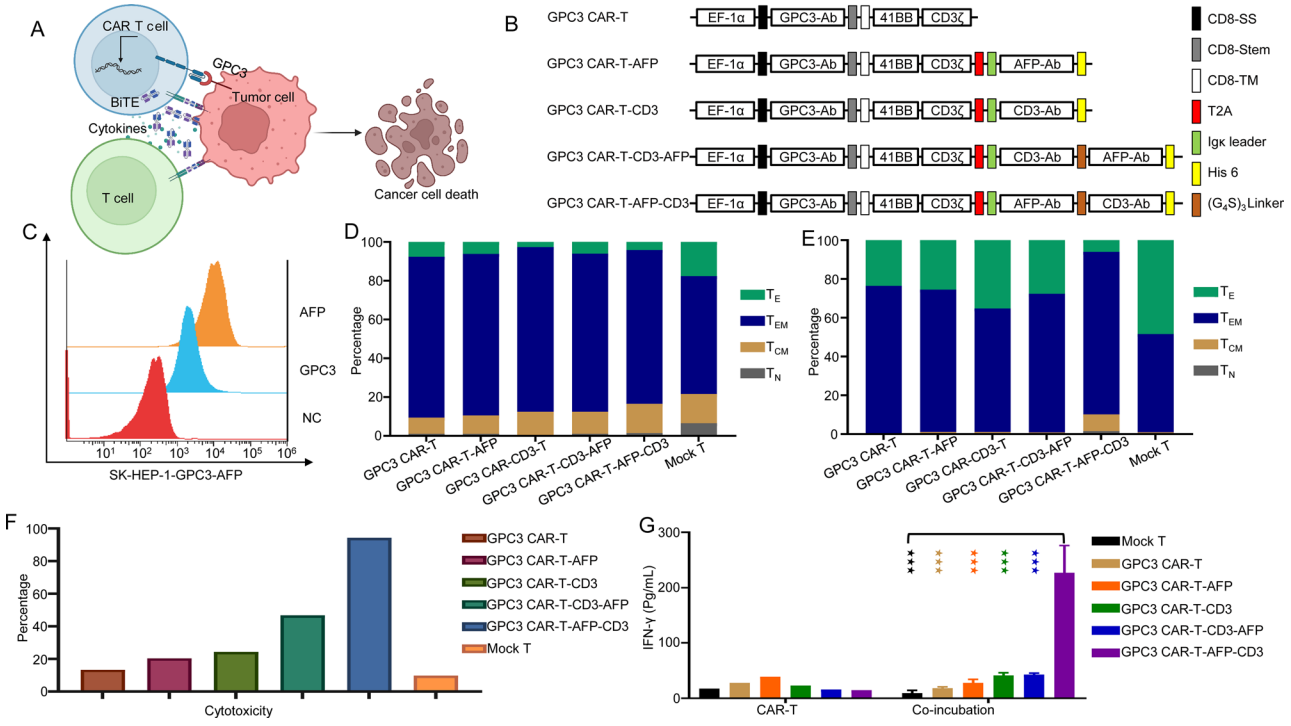

Fig. 6 (**A**) Designed and optimized second-generation GPC3 CAR-T cells that incorporate 4-1BB as a co-stimulatory domain and are capable of secreting BiTE molecules that bind to AFP-expressing tumor cells and T cells. (**B**) Illustration of GPC3 CAR-T/AFP-BiTE construction. (**C**) Confirmation of GPC3 and AFP expression on target liver cancer cell line (SK-HEP-1-GPC3-AFP) by flow cytometry. (**D**) Flow cytometry analysis was performed to detect the memory/effector phenotype of CAR T cells. (**E**) Flow cytometry analysis was performed to detect the memory/effector phenotype of CAR T cells after repeated stimulation experiment in vitro. (**F**) Cytotoxicity of CAR-T Cells in vitro cytotoxicity assay. (**G**) The secretion levels of IFN-γ in both cytotoxicity assays and autocrine secretion of various CAR-T cells

the advantages of both CAR-T and BiTE technologies to improve tumor cell killing, limit antigen escape, and enhance patient outcomes.

Our in vitro and in vivo studies demonstrated the superior efficacy of the dual-targeting CAR-T cells compared to single-target approaches. Transcriptome analysis revealed distinct gene expression profiles in the dual-targeting CAR-T cells, suggesting enhanced DNA damage repair, reduced exhaustion, and increased cytokines and chemokines production.

In summary, the key innovations of our dual-targeting CAR-T strategy including: (1) Novel pMHC Complex Protein Engineering Platform: We established a highly efficient platform for producing pMHC complexes, enabling precise antigen presentation. (2) High-Affinity, Specific AFP Antibody (1B3): We developed the 1B3 antibody, which exhibits strong specificity and high affinity for the AFP antigen. (3) Dual-Targeting CAR-T Cells: We engineered CAR-T cells to target both GPC3 and AFP, leveraging the synergistic effects of these two antigens with tolerated safety and significantly improved antitumor efficacy. (4) Enhanced CAR-T Cell Function: Our dual-targeting CAR-T cells demonstrated superior antitumor activity in vitro and in vivo compared to single-target CAR-T cells. (5) Unique Transcriptomic Profile: Transcriptome analysis revealed distinct gene expression patterns in dual-targeting CAR-T cells, suggesting enhanced DNA damage repair and reduced exhaustion.

In addition, our dual-targeting CAR-T cell therapy offers several advantages: (1) Enhanced Anti-Tumor Efficacy: The combination of two targets increases the likelihood of tumor cell elimination. (2) Reduced Tumor Escape: Dual-targeting can mitigate the risk of tumor cells developing resistance. (3) Enhanced Immune Response: The unique transcriptomic profile of our CAR-T cells suggests improved persistence and function.

While significant progress has been made, challenges remain to be addressed before widespread clinical application of our dual-targeting CAR-T cell therapy for liver cancer. One key hurdle lies in the potential limitation of our therapy to patients expressing both GPC3 and the specific HLA-restricted form of AFP that our platform targets. This could significantly limit the eligible patient population. Further research is crucial to identify additional liver cancer antigens with broader expression patterns, potentially including B7-H3, which is frequently overexpressed in these tumors. By incorporating additional targets into the CAR-T cell design, we can expand the range of patients who can benefit from this therapy.

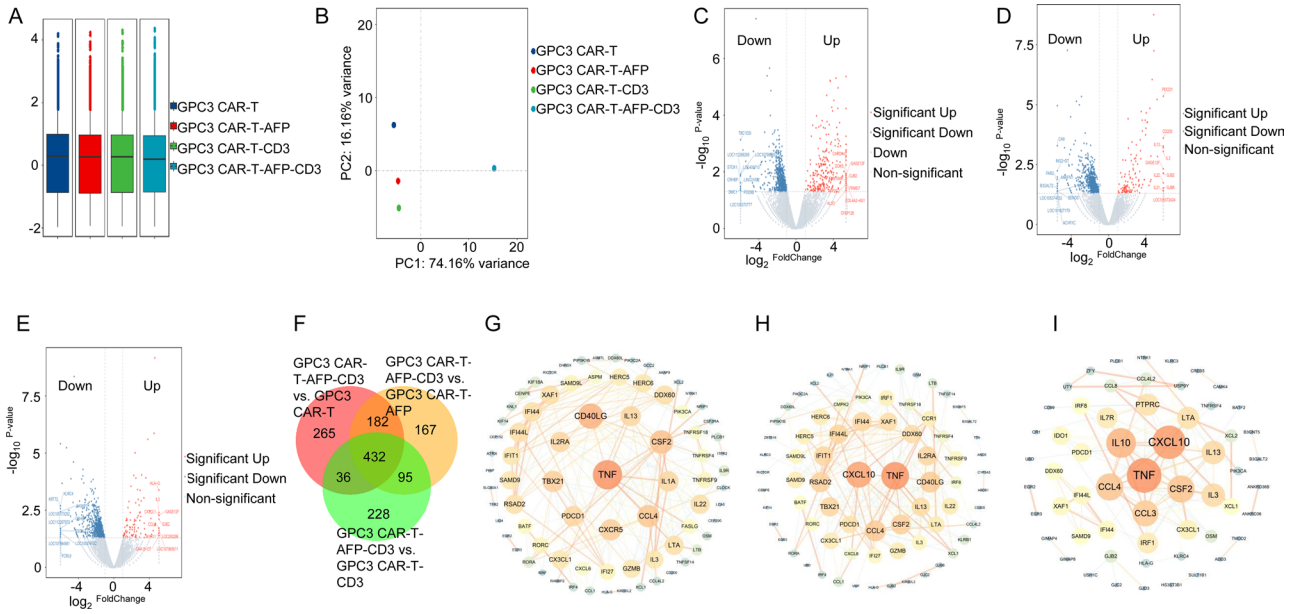

Fig. 7 (**A**) The box plot of gene expression level. (**B**) The principal component analysis of the gene expression of samples in each group. (**C**) The volcano plot of the overall distribution of differentially expressed genes when comparing the GPC3 CAR-T-AFP-CD3 group with the GPC3 CAR-T group; (**D**) The volcano plot of the overall distribution of differentially expressed genes when comparing the GPC3 CAR-T-AFP-CD3 group with the GPC3 CAR-T-AFP group; (**E**) The volcano plot of the overall distribution of differentially expressed genes when comparing the GPC3 CAR-T-AFP-CD3 group with the GPC3 CAR-T-CD3 group. (**F**) The common and unique differentially expressed genes among different comparison groups. (**G**) The PPI network constructed by differentially expressed genes when comparing the GPC3 CAR-T-AFP-CD3 group with the GPC3 CAR-T group. (**H**) The PPI network constructed by differentially expressed genes when comparing the GPC3 CAR-T-AFP-CD3 group with the GPC3 CAR-T-AFP group. (**I**) The PPI network constructed by differentially expressed genes when comparing the GPC3 CAR-T-AFP-CD3 group with the GPC3 CAR-T-CD3 group

Solid tumors, including liver cancer, are notoriously heterogeneous. This means different tumor cells within the same patient can express varying levels of GPC3 and AFP. Additionally, tumor cells can downregulate or lose expression of these antigens altogether over time, a phenomenon known as antigen escape. This heterogeneity and potential for antigen escape can reduce the efficacy of CAR-T therapy. Strategies to develope CAR-T cells with the ability to recognize multiple epitopes within the same target antigen can offer broader targeting capabilities and mitigate the effects of antigen escape.

Furthermore, although no cytokine release syndrome (CRS) associated with persistent CAR-T cell activation was observed in this study, such adverse reactions may vary between individuals and cannot be completely ruled out. The LNP-mRNA-based CAR delivery and expression technology enables transient protein expression, utilizes a non-viral delivery platform (e.g., lipid nanoparticles, LNPs), presents an extremely low risk of transgene integration, and offers versatile therapeutic modalities [36]. This approach effectively circumvents the risks of viral vector-mediated genomic integration inherent in conventional CAR-T technologies and reduces the incidence of CRS to some extent. However, it still requires technical optimization for application in treating certain solid tumors to maintain sustained CAR expression for T cell activation.

While our study suggests improved persistence and function of our dual-targeting CAR-T cells, further research is needed to optimize these aspects. Genetic modifications to CAR-T cells, including the incorporation of co-stimulatory domains or cytokine signaling modules, can enhance their persistence and anti-tumor activity. Additionally, exploring strategies to improve the homing of CAR-T cells to the tumor microenvironment is crucial. This can be achieved by incorporating chemokine receptors or other targeting moieties into the CAR design, allowing for more efficient tumor infiltration and killing. For optimal clinical outcomes, CAR-T therapy may be most effective when combined with other treatment modalities. Pre-conditioning therapies such as chemotherapy or radiation can help to debulk the tumor and create a more favorable microenvironment for CAR-T cell function [37, 38]. Additionally, exploring synergies with checkpoint inhibitors or other immunomodulatory drugs holds promise for further enhancing the anti-tumor response.

In conclusion, our dual-targeting CAR-T cell therapy represents a significant advancement in the field of cancer immunotherapy. By addressing the limitations of single-target CAR-T cells, this approach holds the potential to improve patient outcomes and revolutionize the treatment of liver cancer and other solid tumors.

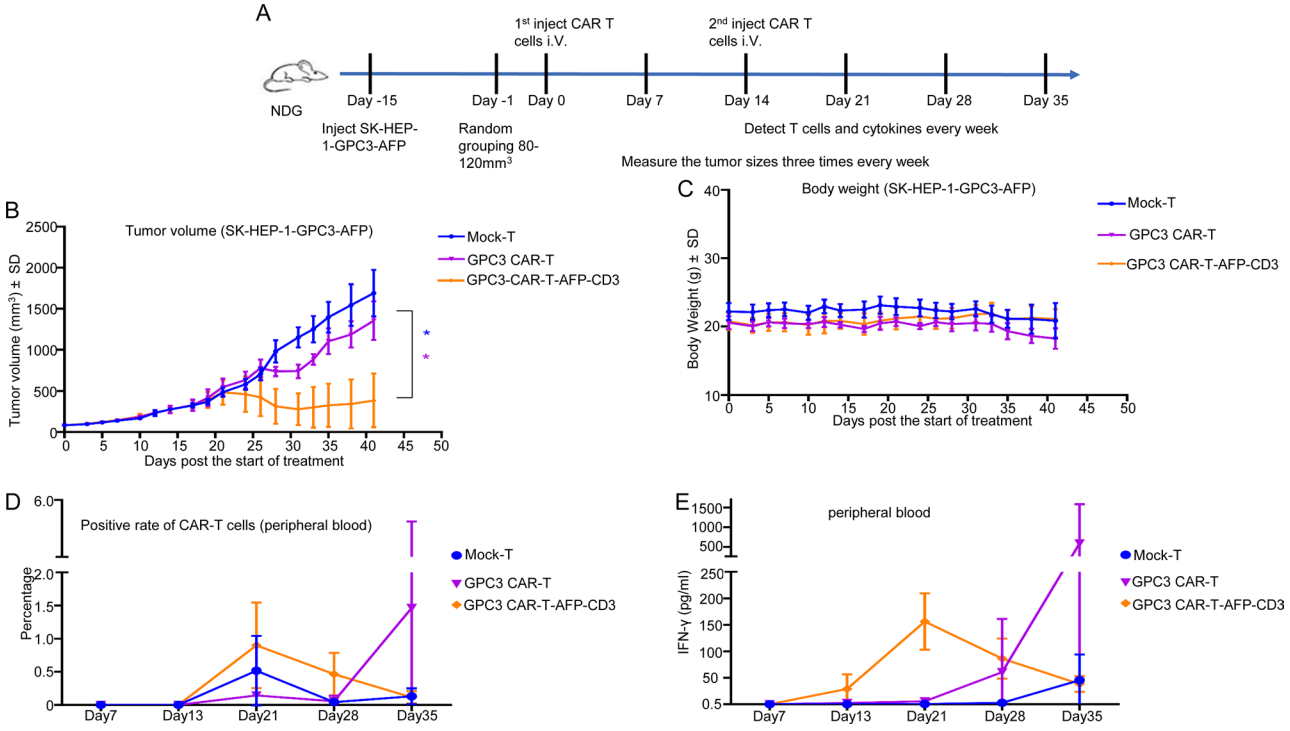

Fig. 8 (**A**) Schematic of the liver cancer xenograft model used to investicate the in vivo activitof CAR-T cells (In this experiment, SK-HEP-1-GPC3-AFP cells were inoculated subcutaneously on Day −15. When tumor volume reached 80–120 mm^3, mice were randomly grouped. The first intravenous administration of CAR-T cells was performed on Day 0, followed by a second intravenous administration on Day 14). NSG mice were subcutaneously injected with 3×10^6 target cells, and CAR-T cells were injected at specified time points. Each group consisted of $n=5$ mice. (**B**) Tumor growth was assessed three times per week following CAR-T cell injection. (**C**) In vivo toxicity was evaluated by monitoring the mice's body weights throughout the treatment. (**D**-**E**) Peripheral blood samples were collected weekly to analyze the levels of $CD3^+$ T cells (**D**) and IFN-γ (**E**)

Supplementary Information

The online version contains supplementary material available at https://doi.org/10.1186/s12951-025-03512-w.

Supplementary Material 1

Supplementary Material 2

Supplementary Material 3

Supplementary Material 4

Supplementary Material 5

Supplementary Material 6

Author contributions

ZY: Conceptualization, Data curation, Writing– original draft. ZLL and CC: Visualization, Investigation. HJW, EMX, XH and BL: Software, Investigation. HWS, JTW, XPL, MMZ, DJL and XWL: Experimental manipulation. XYL, PJ, LGL, XWH, KH, MXZ and WZ: Project administration, Supervision. All authors read and approved the final manuscript.

Funding sources

This work was supported by National Natural Science Foundation of China (Key Program) (Grant No. 82230067), National Natural Science Foundation of China (General Program) (Grant No. 82272103), Natural Science Foundation of Guangdong Province for Distinguished Young Scholars (Grant No. 2022B1515020010), Shanghai Pujiang Program (23PJ1423800), Guangzhou Municipal Science and Technology Program Project (Grant No. 2025A03J4320), Special Project for Clinical and Basic Sci&Tech Innovation of Guangdong Medical University (Grant No. GDMULCJC2024128), The Natural Science Foundation of Guangdong Province of China (Grant No. 2021A1515220183), Guangdong Provincial Medical Science and Technology Research Fund Project (Grant No. A2023492), Guangzhou Science and Technology Plan Project (Grant No. 2024A03J0133) and National Natural Science Foundation of China (Youth Science Fund Project) (Grant No. 82202829).

Data availability

No datasets were generated or analysed during the current study.

Declarations

Ethics approval

All individuals provided informed consent to participate in this study and approval was provided by the Ethics Committee of Drug Clinical Experiment of Zhejiang Xiaoshan Hospital. Animal care and experiments were performed in accordance with institutional and national guidelines. All animal experiments were performed in accordance with a protocol approved by Animal Research Committee of Shanghai YouShu Life Technology CO., LTD.

Competing interests

The authors declare no competing interests.

Author details

[1]Interventional Medical Treatment Department, Guangzhou First Pepople's Hospital, the Second Affiliated Hospital, School of Medicine, South China University of Technology, Guangzhou, China
[2]The Affiliated Dongguan Songshan Lake Central Hospital, Guangdong Medical University, Dongguan, China
[3]Guangdong Provincial Key Laboratory of Tumor Interventional Diagnosis and Treatment, Zhuhai People's Hospital (Zhuhai Clinical Medical College of Jinan University), Zhuhai, China
[4]R&D Department, OriCell Therapeutics Co. Ltd, Shanghai, China
[5]Department of Biomedical Sciences, Faculty of Health Sciences, University of Macau, Macau, China

[6]Minimally Invasive Tumor Therapies Center, The Affiliated Guangdong Second Provincial General Hospital of Jinan University, Guangzhou, China

Received: 15 December 2024 / Accepted: 28 May 2025
Published online: 24 June 2025

References

1. Zheng R, Zhang S, Zeng H, Wang S, Sun K, Chen R, et al. Cancer incidence and mortality in china, 2016. J Natl Cancer Cent. 2022;2(1):1–9.
2. Zheng RS, Zhang SW, Sun KX, Chen R, Wang SM, Li L, et al. [Cancer statistics in china, 2016]. Zhonghua Zhong Liu Za Zhi. 2023;45(3):212–20.
3. Siegel RL, Giaquinto AN, Jemal A. Cancer statistics, 2024. CA Cancer J Clin. 2024;74(1):12–49.
4. Du J, Su Y, Gao J, Tai Y. The expression and function of long noncoding RNAs in hepatocellular carcinoma. Cancer Innov. 2023;2(6):488–99.
5. Finn RS, Qin S, Ikeda M, Galle PR, Ducreux M, Kim TY, et al. Atezolizumab plus bevacizumab in unresectable hepatocellular carcinoma. N Engl J Med. 2020;382(20):1894–905.
6. Finn RS, Qin S, Ikeda M, Galle PR, Ducreux M, Kim T-Y et al. IMbrave150: Updated overall survival (OS) data from a global, randomized, open-label phase III study of atezolizumab (atezo) + bevacizumab (bev) versus sorafenib (sor) in patients (pts) with unresectable hepatocellular carcinoma (HCC). J Clin Oncol. 2021;39(3_suppl):267.
7. Zhang L, Liu R, Deng T, Ba Y. Advances in medical treatment of advanced hepatobiliary and pancreatic cancer in 2022. Cancer Innov. 2023;2(1):36–51.
8. Galle PR, Finn RS, Qin S, Ikeda M, Zhu AX, Kim TY, et al. Patient-reported outcomes with Atezolizumab plus bevacizumab versus Sorafenib in patients with unresectable hepatocellular carcinoma (IMbrave150): an open-label, randomised, phase 3 trial. Lancet Oncol. 2021;22(7):991–1001.
9. Yau T, Kang YK, Kim TY, El-Khoueiry AB, Santoro A, Sangro B, et al. Efficacy and safety of nivolumab plus ipilimumab in patients with advanced hepatocellular carcinoma previously treated with sorafenib: the checkmate 040 randomized clinical trial. JAMA Oncol. 2020;6(11):e204564.
10. Zhu AX, Finn RS, Edeline J, Cattan S, Ogasawara S, Palmer D, et al. Pembrolizumab in patients with advanced hepatocellular carcinoma previously treated with Sorafenib (KEYNOTE-224): a non-randomised, open-label phase 2 trial. Lancet Oncol; 2018. pp. 940–52.
11. Schepers EJ, Glaser K, Zwolshen HM, Hartman SJ, Bondoc AJ. Structural and functional impact of posttranslational modification of Glypican-3 on liver carcinogenesis. Cancer Res. 2023;83(12):1933–40.
12. Shi DH, Shi YP, Kaseb AO, Qi XX, Zhang Y, Chi JC, et al. Chimeric antigen Receptor-Glypican-3 T-Cell therapy for advanced hepatocellular carcinoma: results of phase I trials. Clin Cancer Res. 2020;26(15):3979–89.
13. Shi YP, Shi DH, Chi JC, Cui D, Tang XY, Lin Y, et al. Combined local therapy and CAR-GPC3 T-cell therapy in advanced hepatocellular carcinoma: a proof-of-concept treatment strategy. Cancer Commun. 2023;43(9):1064–8.
14. Zhao Z, Guo W, Fang S, Song S, Song J, Teng F, et al. An armored GPC3-directed CAR-T for refractory or relapsed hepatocellular carcinoma in china: A phase I trial. J Clin Oncol. 2021;39(15suppl):4095.
15. Zhao Z, Ji J, He X, Ding X, Tang Y, Feng X et al. A Phase I open-label clinical study evaluating the safety, pharmacokinetics, and preliminary efficacy of targeted GPC3 chimeric antigen receptor autologous T-cell infusion therapy (Ori-C101) in patients with failed advanced hepatocellular carcinoma (HCC). 25th Annual Meeting of Chinese Society of Clinical Oncology; September 21st to 26th, 2022; Bei Jing, Shang Hai, Guang Zhou, Ji Nan: Journal of Clinical Oncology; 2022. pp. 150-1. (in Chinese).
16. Hu X, Chen R, Wei Q, Xu X. The landscape of alpha Fetoprotein in hepatocellular carcinoma: where are we? Int J Biol Sci. 2022;18(2):536–51.
17. Butterfield LH, Meng WS, Koh A, Vollmer CM, Ribas A, Dissette VB, et al. T cell responses to HLA-A*0201-restricted peptides derived from human alpha Fetoprotein. J Immunol. 2001;166(8):5300–8.
18. Butterfield LH, Ribas A, Meng WS, Dissette VB, Amarnani S, Vu HT, et al. T-cell responses to HLA-A*0201 immunodominant peptides derived from alpha-fetoprotein in patients with hepatocellular cancer. Clin Cancer Res. 2003;9(16 Pt 1):5902–8.
19. Pichard V, Royer PJ, Richou C, Cauchin E, Goebes K, Gaignerie A, et al. Detection, isolation, and characterization of alpha-fetoprotein-specific T cell populations and clones using MHC class I multimer magnetic sorting. J Immunother. 2008;31(3):246–53.
20. Akahori Y, Wang L, Yoneyama M, Seo N, Okumura S, Miyahara Y, et al. Antitumor activity of CAR-T cells targeting the intracellular oncoprotein WT1 can be enhanced by vaccination. Blood. 2018;132(11):1134–45.
21. Liu H, Xu Y, Xiang J, Long L, Green S, Yang Z, et al. Targeting Alpha-Fetoprotein (AFP)-MHC complex with CAR T-Cell therapy for liver Cancer. Clin Cancer Res. 2017;23(2):478–88.
22. Sun Y, Wu P, Zhang Z, Wang Z, Zhou K, Song M et al. Integrated multi-omics profiling to dissect the Spatiotemporal evolution of metastatic hepatocellular carcinoma. Cancer Cell. 2023.
23. Calderaro J, Ziol M, Paradis V, Zucman-Rossi J. Molecular and histological correlations in liver cancer. J Hepatol. 2019;71(3):616–30.
24. Craig AJ, von Felden J, Garcia-Lezana T, Sarcognato S, Villanueva A. Tumour evolution in hepatocellular carcinoma. Nat Rev Gastroenterol Hepatol. 2020;17(3):139–52.
25. Nasiri F, Farrokhi K, Safarzadeh Kozani P, Mahboubi Kancha M, Dashti Shokoohi S. Safarzadeh Kozani P. CAR-T cell immunotherapy for ovarian cancer: hushing the silent killer. Front Immunol. 2023;14:1302307.
26. Goebeler ME, Bargou RC. T cell-engaging therapies - BiTEs and beyond. Nat Rev Clin Oncol. 2020;17(7):418–34.
27. Kegyes D, Constantinescu C, Vrancken L, Rasche L, Gregoire C, Tigu B, et al. Patient selection for CAR T or bite therapy in multiple myeloma: which treatment for each patient? J Hematol Oncol. 2022;15(1):78.
28. Yin Y, Rodriguez JL, Li N, Thokala R, Nasrallah MP, Hu L, et al. Locally secreted bites complement CAR T cells by enhancing killing of antigen heterogeneous solid tumors. Mol Ther. 2022;30(7):2537–53.
29. Heidbuechel JPW, Engeland CE. Oncolytic viruses encoding bispecific T cell engagers: a blueprint for emerging immunovirotherapies. J Hematol Oncol. 2021;14(1):63.
30. Brudno JN, Maus MV, Hinrichs CS. CAR T cells and T-Cell therapies for cancer: A translational science review. JAMA. 2024;74840098. https://doi.org/10.1001/jama.2024.19462.
31. Ai K, Liu B, Chen X, Huang C, Yang L, Zhang W, et al. Optimizing CAR-T cell therapy for solid tumors: current challenges and potential strategies. J Hematol Oncol. 2024;17(1):105.
32. Ash SL, Orha R, Mole H, Dinesh-Kumar M, Lee SP, Turrell FK et al. Targeting the activated microenvironment with endosialin (CD248)-directed CAR-T cells ablates perivascular cells to impair tumor growth and metastasis. J Immunother Cancer. 2024;12(2).
33. Dharani S, Cho H, Fernandez JP, Juillerat A, Valton J, Duchateau P, et al. TALEN-edited allogeneic inducible dual CAR T cells enable effective targeting of solid tumors while mitigating off-tumor toxicity. Mol Ther. 2024;S1525–0016(24):00540–9.
34. Erler P, Kurcon T, Cho H, Skinner J, Dixon C, Grudman S, et al. Multi-armored allogeneic MUC1 CAR T cells enhance efficacy and safety in triple-negative breast cancer. Sci Adv. 2024;10(35):eadn9857.
35. Liu L, Bi E, Ma X, Xiong W, Qian J, Ye L, et al. Enhanced CAR-T activity against established tumors by polarizing human T cells to secrete interleukin-9. Nat Commun. 2020;11(1):5902.
36. Li Y, Tian Y, Li C, Fang W, Li X, Jing Z, et al. In situ engineering of mRNA-CAR T cells using spleen-targeted ionizable lipid nanoparticles to eliminate cancer cells. Nano Today. 2024;59:102518.
37. Ward MB, Jones AB, Krenciute G. Therapeutic advantage of combinatorial CAR T cell and chemo-therapies. Pharmacol Rev. 2024:PHARMREV-AR-2023-001070.
38. Hovhannisyan L, Riether C, Aebersold DM, Medová M, Zimmer Y. CAR T cell-based immunotherapy and radiation therapy: potential, promises and risks. Mol Cancer. 2023;22(1):82.

Publisher's note